Chemical Engineering Journal 144 (2008) 270–276

Contents lists available at ScienceDirect

Chemical Engineering Journal

journal homepage: www.elsevier.com/locate/cej

Catalytic combustion of methane over Pd-based catalyst supported on a macroporous alumina layer in a microchannel reactor

Guoqing Guan [a], Katsuki Kusakabe [a,*], Masatsugu Taneda [a], Masato Uehara [b], Hideaki Maeda [b]

[a] Department of Living Environmental Science, Fukuoka Women's University, 1-1-1 Kasumigaoka, Higashi-ku, Fukuoka 813-8529, Japan
[b] Nanotechnology Research Institute, National Institute of Advanced Industrial Science and Technology (AIST), 807-1 Shuku-machi, Tosu, Saga 841-0052, Japan

ARTICLE INFO

Article history:
Received 11 March 2008
Received in revised form 17 May 2008
Accepted 4 June 2008

Keywords:
Methane combustion
Microchannel reactor
Pd-based catalyst
Inverse opal structure
Random macroporous structure
Wash-coating

ABSTRACT

Catalytic combustion of high concentrations of methane over Pd-loaded γ-Al_2O_3 catalysts coated in microchannels was investigated. Three types of γ-Al_2O_3 coating structures were prepared in microchannels: a well defined ordered macroporous structure (inverse opal structure), a random macroporous structure and a structure without macropores (dense structure). Pd-based catalysts were loaded on the prepared coatings using the incipient wetness impregnation method. Test results for the catalytic combustion of methane indicated that the catalysts supported on coatings with an ordered or random macroporous structure showed better reactive activity than those on coatings with a dense structure.

1. Introduction

Natural gas, which is composed mainly of methane, has recently attracted attention because it combusts with less byproducts compared to other fuels. Flame combustion [1,2] and catalytic combustion [3,4] have been performed to produce thermal energy. Catalytic combustion has very attractive characteristics compared with flame combustion. The combustion temperature is lower and combustion is performed at a concentration range outside of flammability limits, due to the complete oxidation property. As a result, almost no NO_x, CO or particulate matter can be observed.

Integrated microchemical systems for fuel processing applications have been widely studied in recent years [5,6]. Catalytic combustion of methane in a conventional fixed-bed reactor has been widely studied [7–16]. However, methane concentration in the feed gas is usually as low as 1.0 vol.% due to the explosive limit of methane, in the range of 5–15 vol.% in air. In a microchannel combustion system used as a heat source for other microdevices, catalytic combustion at relatively high concentration is needed. In this particular case, a reactor could minimize the possibility of explosion, due to its small reactor volume [5].

The catalysts for methane combustion can be divided into two groups, noble metals such as Pt, Pd, Rh, and Ru, and transition metal oxides such as Co_3O_4, CuO, Cr_2O_3 and MnO_2. Transition metal oxides show catalytic activity at relatively high temperatures (>700 °C), and thus are not suitable for use in stainless steel microreactors due to low operating temperature limits. Among the noble metal-based catalysts, the activities of Pd and Pt are considered to be significantly higher than the others, and Pd-based catalysts always show the best activity in methane combustion [17]. The effects of porous ceramic supports, such as Al_2O_3, SiO_2, SiO_2–Al_2O_3, ZrO_2, SnO_2 and TiO_2, on catalytic activity have also been extensively studied. The most common catalyst for methane combustion at low temperatures is Pd loaded γ-Al_2O_3 catalyst. It has been reported that PdO was active in methane combustion, whereas Pd was less active, and the interaction between PdO and alumina considerably improved thermal stability in the oxidizing atmosphere [18–20].

In a microchannel reactor, the catalyst support should be coated on the surface of the microchannel. To date, wash-coating and dip-coating have been the most common methods. Using these methods, a dense catalyst-coating layer could be successfully formed on the wall of a microchannel [21,22]. In order to increase the area of contact between the catalysts and reactants in the small space, some improved methods have also been proposed. For instance, Kenis and co-workers [23–25] developed a method for the preparation of SiCN and/or SiC catalyst supports with inverse opal structure in microchannels, and used the catalysts for ammonia decomposition and propane steam reforming to produce hydrogen for a fuel cell. Mo-promoted Pt catalyst supported on the Al_2O_3

* Corresponding author. Tel.: +81 92 682 1733; fax: +81 92 682 1733.
E-mail address: kusakabe@fwu.ac.jp (K. Kusakabe).

1385-8947/$ – see front matter © 2008 Elsevier B.V. All rights reserved.
doi:10.1016/j.cej.2008.06.001

inverse opal structure showed excellent reactivity for propane combustion in the microchannel reactor [26]. The Al_2O_3 inverse opal structure was formed by a process in which Al_2O_3 in the voidage around a hexagonal polymer sphere packing with the spheres afterwards burnt out. However, it was found that the inverse opal structures prepared in the microchannel did not strongly adhere to the wall of the channel. The inverse opal structure had to be reinforced by the addition of ceramic glue to enhance the adhesive properties. In the present study, we coated a macroporous γ-Al_2O_3 support layer in the microchannel using two methods: infiltration of γ-Al_2O_3 sol into the opal structures formed in the microchannel, which is the same process reported in the literature [26], and direct coating of a suspension composed of uniform template polymer particles, γ-Al_2O_3 ceramic nanoparticles and binding materials. Pd-based catalysts were loaded on the support layer using the incipient wetness impregnation method. Catalytic reaction tests for methane combustion using the Pd-based catalysts with the two kinds of macroporous structures were then performed, and the results were compared with a catalyst system without a macroporous structure, prepared by a wash coating method.

2. Experimental

2.1. Design of the microchannel reactor

The microreactor design was composed of two stainless steel plates with microchannels, which were jacketed in a stainless steel cell as shown in Fig. 1. Each plate had 14 microchannels of 25 mm long, with a semicircular cross-section (500 μm wide, 250 μm deep). Accordingly, the cross-sectional shape of the microchannel was circular. Before preparation of the coatings in the microchannels, the plates were cleaned and thermally treated at 800 °C for 2 h, followed by clean treatment with distilled water and acetone.

2.2. Preparation of Al_2O_3 supports in the microchannel

2.2.1. Preparation of Al_2O_3 support with random macropores

As shown in Fig. 2(a), 0.5 g of PMMA particles (Soken Chemical and Engineering Co., Japan) 310 nm in size were dispersed in 4 ml of distilled water containing 6 wt.% of polyvinyl alcohol (PVA, Fluka). Then 0.5 g of γ-Al_2O_3 nanoparticles (Alfar Aesar, particle size = 8–14 nm) were dispersed into the mixture under stirring. After 24 h stirring at room temperature, the resulting suspension was introduced into the microchannels. It was found that the suspension could be moved along the microchannel automatically by capillary force from one side to the other. The coated plates were dried at 90 °C for 12 h and then heated to 300 °C in air and kept at this temperature for 2 h to burn out the PMMA particles. In order to remove all the organic components, the plates were further calcinated at 600 °C for 3 h.

2.2.2. Preparation of Al_2O_3 support with inverse opal structure

The inverse opal structure of γ-Al_2O_3 was prepared according to the method used in a previous paper [26]. As shown in Fig. 2(b), 10 wt.% of PMMA colloidal suspension was introduced into the microchannel. When water in the suspension was evaporated at room temperature, PMMA opals with well-defined structures were formed in the microchannels. PMMA particle-packed microchannels were heated at 90 °C for 24 h in order to improve connectivity between the neighboring particles.

Aluminum sol was prepared by dilution of 2 ml of aluminum-tri-*sec*-butylate (Aldrich) in 4 ml of absolute ethanol and then stirred in a capped bottle for 15 min, followed by addition of 1 ml of a mixture of acetylacetone (Aldrich) and ethylacetoacetate (Aldrich) with a molar ratio of 1:4 as stabilizer. After stirring for 2 h, a concentrated nitric acid solution (69%, Wako) was added drop by drop to adjust

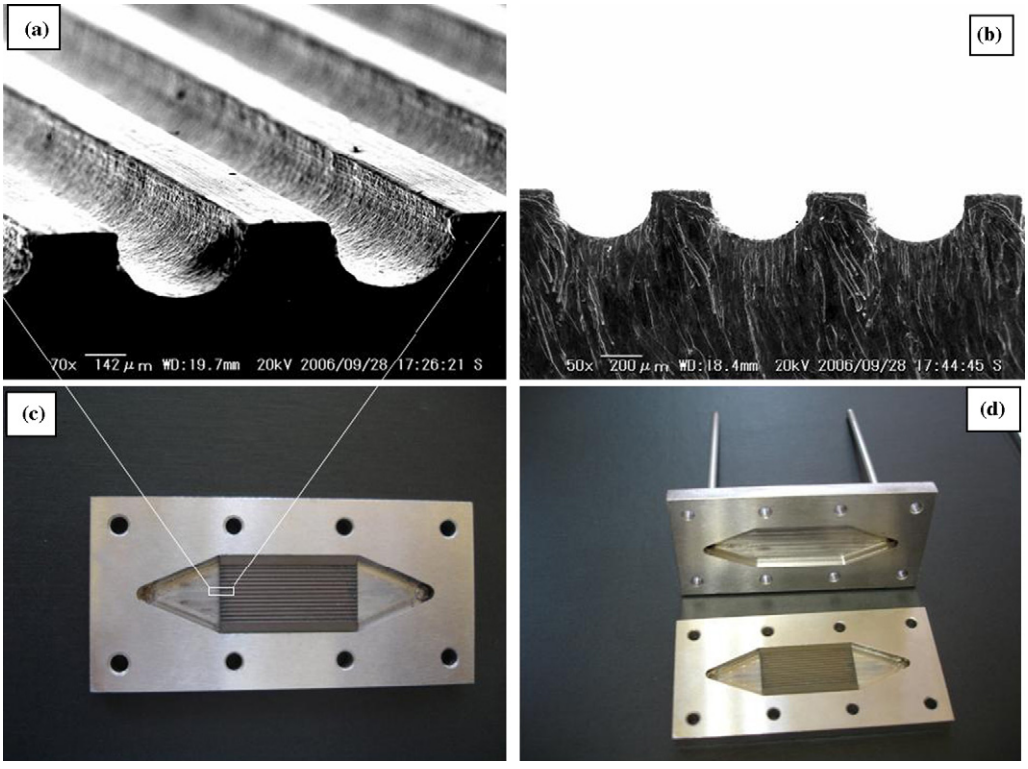

Fig. 1. Microchannel and its jackets. (a) Microchannel; (b) cross-section of microchannel; (c) microchannel in the jacket; (d) jackets.

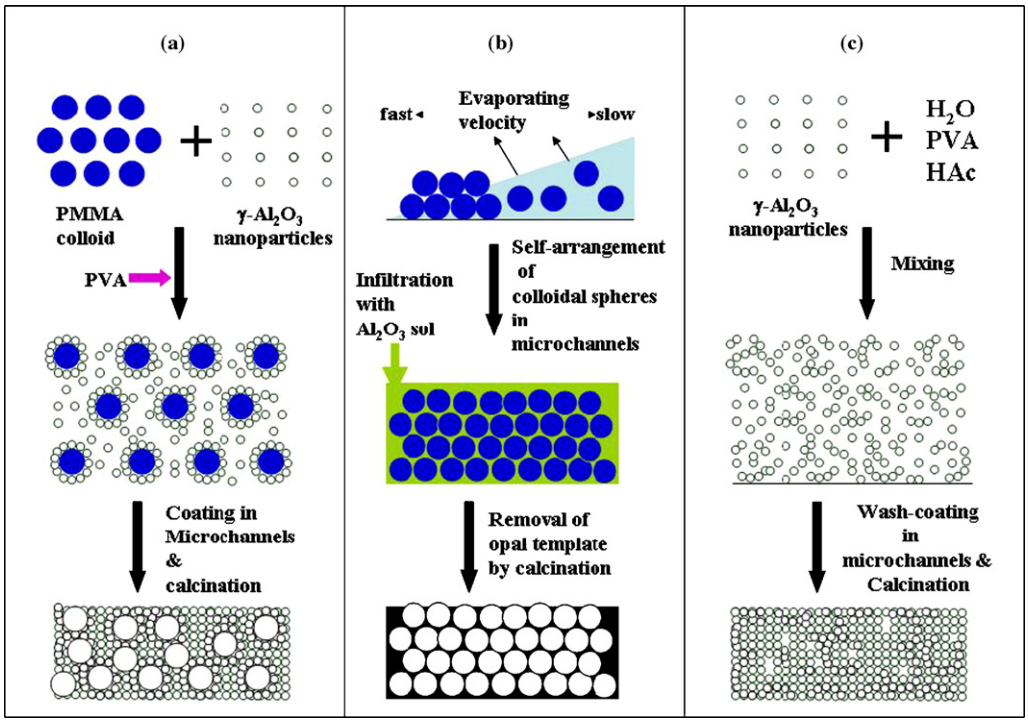

Fig. 2. Coating methods for the preparation of supports in the microchannels. (a) Coatings with random macropores; (b) coatings with well-defined macropores; (c) coatings without macropores.

the pH value to 4.5. A stable clear sol was obtained. The prepared Al_2O_3 sol was then infiltrated into the void in the PMMA opals in a nitrogen-purged glove box. The infiltration process was repeated several times due to the low concentration of the Al_2O_3 sol. The heat treatment procedures were the same as those described above. Due to the shrinkage effect, the cracks that formed were restored by carefully filling of a small amount of Al_2O_3 suspension composed of Al_2O_3 nanoparticles, polyvinyl alcohol and water [26].

2.2.3. Preparation of Al_2O_3 support without macropores

As shown in Fig. 2(c), γ-Al_2O_3 nanoparticles were dispersed in a solution containing 6 wt.% PVA and 2 wt.% acetic acid under stirring. The obtained suspension was wash-coated in the microchannels using a method reported in the literature [21]. The calcination methods for the wash-coated plates were the same as those described above.

2.3. Impregnation of catalysts

Incipient wetness impregnation of Pd catalyst on the porous Al_2O_3 support layer in the microchannels was performed as follows: a calculated amount of aqueous solution of $Pd(NO_3)_2$ based on the weight of the Al_2O_3 layer was dropped into the layer, followed by drying at 120 °C for 12 h, and was then calcinated at 500 °C for 3 h. The Pd catalyst loaded on the Al_2O_3 layer in the microchannels was obtained in this manner. In this study, 1.0, 2.5, and 5.0 wt.% Pd-loaded catalysts were prepared.

2.4. Characterization

The morphologies of the prepared coatings were observed with a scanning electron microscope (SEM, Hitachi, S-5200). Powder X-ray diffraction (XRD) patterns of the catalysts were recorded on a Rigaku RINT-2500 diffractometer using Cu Kα radiation

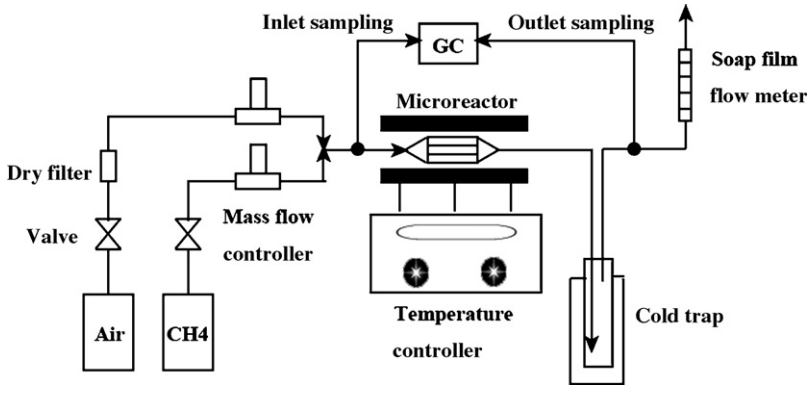

Fig. 3. Schematic diagram of the methane combustion set-up.

(λ = 0.15418 nm) generated at 40 kV and 30 mA. Nitrogen absorption/desorption isotherm measurements were done at 77 K on a Micrometritics ASAP 2010 gas sorptometer. Prior to the measurements, the samples were degassed at 120 °C for 12 h.

2.5. Catalytic reaction

Two plates with catalyst coatings were jacketed tightly using two jackets, as shown in Fig. 1(d). A schematic diagram of the methane combustion set-up is shown in Fig. 3. The reaction was performed at isothermal conditions, and the reactor temperature was controlled by a thermocouple attached to the microreactor. The gas flow rates of methane and air were controlled by mass flow controllers. CH_4 concentrations in the feed gas stream were 9.5, 6.0, 5.0 and 4.0%. The feed gas was introduced into the microreactor at the total flow rates of 30, 60 and 90 ml (STP) min^{-1}. After condensation of the produced water by an ice trap, CO, CO_2 and CH_4 in the effluent dry gases were analyzed by a gas chromatograph (GC-8A, Shimadzu) equipped with a flame ionization detector. In order to detect low levels of CO and CO_2, a methanizer (MT221, GL Sciences) packed with a nickel catalyst powder was installed on the gas line before the FID detector. H_2 was analyzed simultaneously by a gas chromatograph (GC-8A, Shimadzu) equipped with a thermal conductivity detector.

3. Results and discussion

Fig. 4(a) and (c) shows SEM images of prepared γ-Al_2O_3 supports with random and ordered macroporous structures, respectively. Fig. 4(d) shows the γ-Al_2O_3 supports without macropores, prepared by the wash-coating method. Fig. 4(b) shows the self-arranged PMMA particles with close-packed opal structure in the microchannel before the support with the inverse opal structure was prepared. The macroporous γ-Al_2O_3 support with a regular hexagonal structure was formed (Fig. 4(c)), indicating that the well defined ordered PMMA template was well replicated. The pores connected to the deep layer can be also clearly seen. Theoretically, the total porosity of the ordered macroporous structure is as high as 74%, and it can have advantages when used as a catalyst support. However, it was found that this structure had low mechanical strength, and cracks were very easily formed due to the shrinkage (ca. 19%) of the infiltrated sol, as well as shrinkage of the polymer particles used during calcination. Therefore, a post-treatment must be performed, as described in the experimental section.

A macroporous γ-Al_2O_3 support with a random structure (Fig. 4(a)) was formed in the microchannels when the method suggested in Fig. 2 (a) was used. The pores were uniform and spherical in shape, with a pore diameter of ca. 300 nm, which is smaller than the raw PMMA spheres (310 nm) due to shrinkage of the polymer and sintering of the nanoparticles. Few cracks were formed along the whole microchannel, due to the utilization of nanoparticles as infiltration materials, which was expected to lead to less shrinkage than the sol. The total porosity of the coating layer was ca. 70% in the present study, which could be advantageous for use as a catalyst support. In addition, the wall thickness of the pores was greater than that of the inverse opal structure, and as a result, the mechanical strength and adhesion force to the surface of the microchannel were enhanced. The procedure to prepare an alumina support with a random macroporous structure is cost-effective and timesaving. A similar procedure has recently been used to prepare random macroporous yttria stabilized zirconia (YSZ)-based composites for solid oxide fuel cell (SOFC) applications [27]. This method improved the performance of SOFC electrode materials. Tang et al. [28–30] used a similar process for the fabrication of macroporous α-Al_2O_3, TiO_2 and ZrO_2 materials, but no application results were reported. Obviously, a catalyst support with a macroporous structure could provide a wide surface area for the catalytic reaction in a microchannel reactor. As shown in Fig. 4(d), a dense layer with random micropores was formed when using wash-coating method.

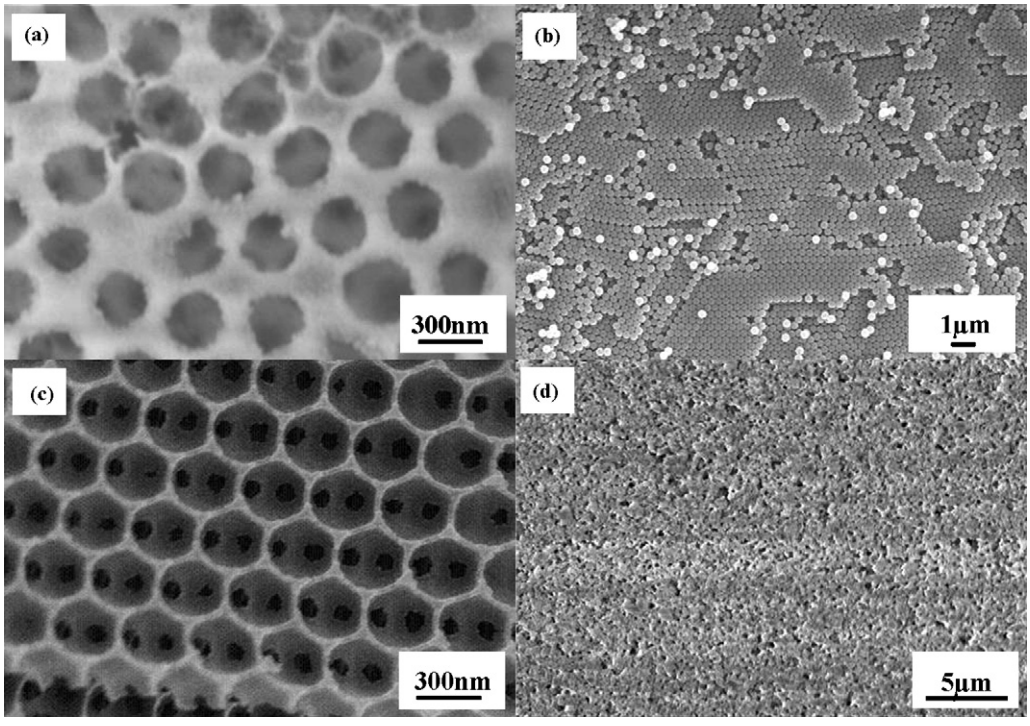

Fig. 4. SEM images of prepared γ-Al_2O_3 coatings in the microchannels. (a) Coating with random macropores; (b) PMMA opals in the microchannel; (c) coating with well-defined ordered macropores; (d) coating without uniform macropores.

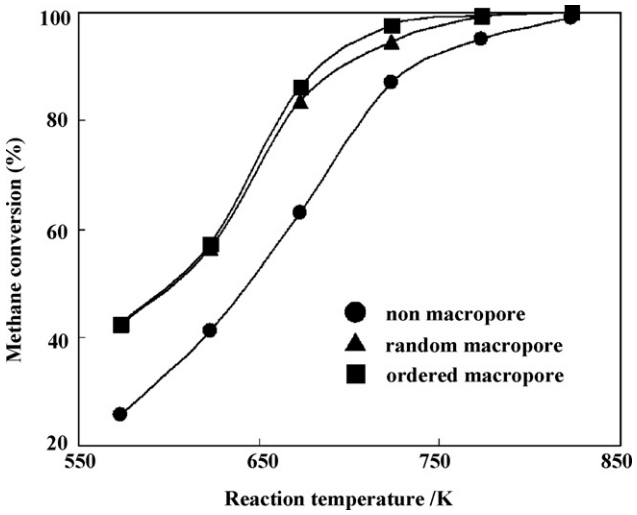

Fig. 5. Methane conversion over 5 wt.% Pd/Al_2O_3 catalysts with ordered and random macroporous structures and without macroporous structure as a function of the reaction temperature. WHSV = 15,200 $dm^3\ h^{-1}\ g_{cat}{}^{-1}$.

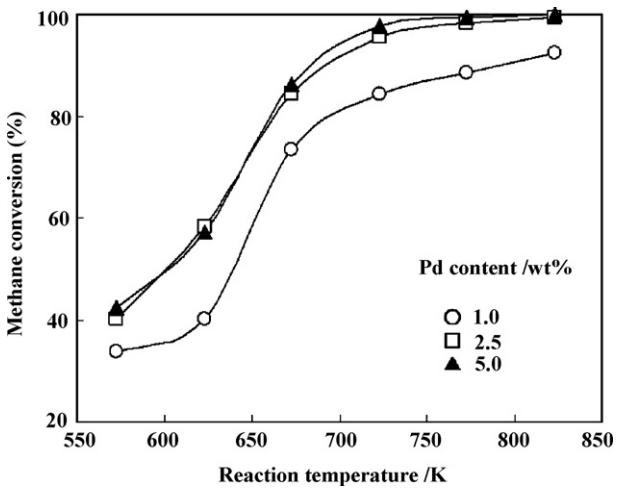

Fig. 7. Methane conversion over Pd/Al_2O_3 catalyst with random macroporous structure as a function of reaction temperature with different Pd contents. WHSV = 15,200 $dm^3\ h^{-1}\ g_{cat}{}^{-1}$.

The steady-state methane conversions over 5 wt.% Pd/Al_2O_3 catalysts with ordered and random macroporous structures and without macroporous structure, as a function of the reaction temperature, are shown in Fig. 5. Elapsed time of 30 min was enough to attain a steady state, judging from the data on product composition. No carbon monoxide was detected in any of the experimental conditions. Methane conversions for the catalysts with ordered and random macroporous structures were almost the same, regardless of porosity differences. Judging from the results obtained by the three catalysts, the introduction of macropores in the catalyst structure highly enhanced the reactivity of methane combustion. The microchannel reactor itself can be designed to provide rapid mass transfer due to a short diffusion length. Furthermore, the introduction of macropores on the microchannel wall surface increased the contact area for the reaction gas and coated catalysts. This could be especially beneficial for fast gas-solid reactions such as methane oxidation.

The methane concentrations for the combustion systems in the literature [7–16] were always kept below 3 vol.% in order to avoid possible explosive problems. In the present study, the methane concentration in the inlet gas mixture was as high as 9.5 vol.%, which is in the range of methane explosive limits (5–10 vol.%), but the appearing reaction process was just the controlled oxidation of methane. This suggests that the mixtures of methane and air were safely handled due to the high heat transfer rates and the explosion inhibiting dimensions of the microchannels. Thus, the methane could be completely converted without explosions by maintaining a heterogeneous catalytic reaction using the designed microchannel reactor.

Fig. 6 shows methane conversion over 5 wt.% Pd/Al_2O_3 catalyst with a random macroporous structure under conditions with different space velocities. When the weight hourly space velocity (WHSV) of the gas phase was below 7600 $dm^3\ h^{-1}\ g_{cat}{}^{-1}$, methane could be completely converted to CO_2 and H_2O at 500 °C with a residence time above 69 ms in the microreactor. When the WHSV increased to 15,200 $dm^3\ h^{-1}\ g_{cat}{}^{-1}$ with a residence time below 46 ms, the temperature of complete methane conversion increased to above 550 °C. This phenomenon is similar to that of propane combustion in the microchannel reactor [26]. When the methane concentration was decreased to 4.0% at 550 °C and the WHSV was 15,200 $dm^3\ h^{-1}\ g_{cat}{}^{-1}$, methane conversion was decreased to 91%.

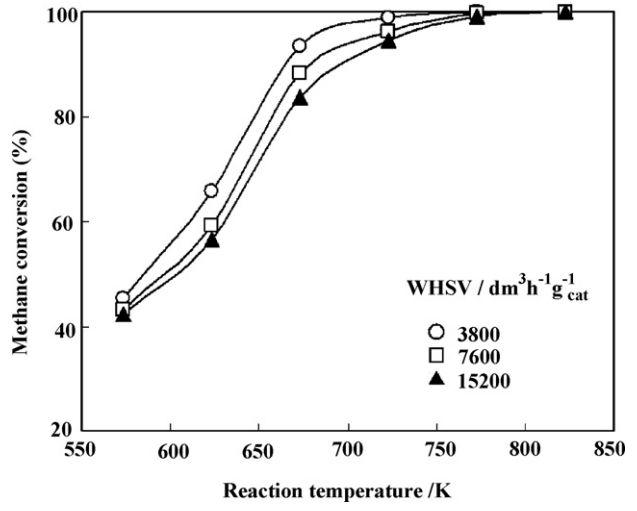

Fig. 6. Methane conversion over 5 wt.% Pd/Al_2O_3 catalyst with random macroporous structure as a function of reaction temperature at various space velocities.

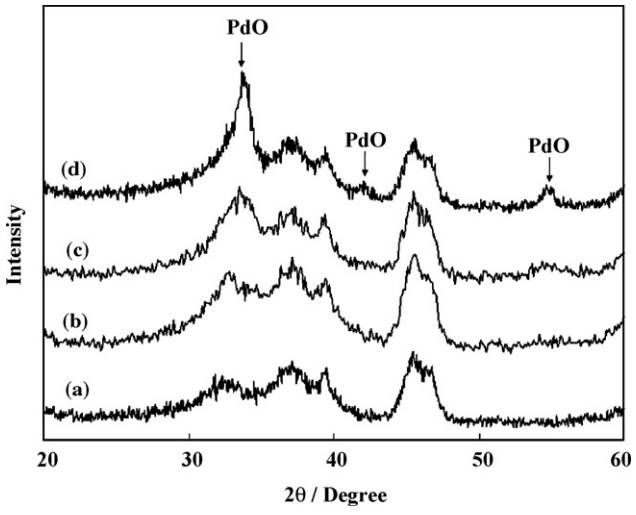

Fig. 8. XRD patterns of (a) Al_2O_3; (b) 1.0 wt.% Pd/Al_2O_3; (c) 2.5 wt.% Pd/Al_2O_3 and (d) 5.0 wt.% Pd/Al_2O_3 with random macroporous structure.

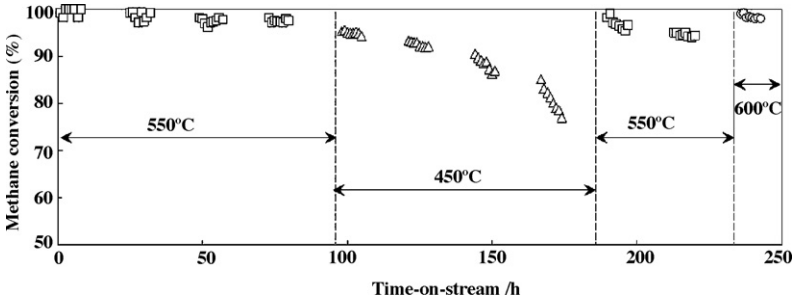

Fig. 9. Long-term stability test for methane combustion over 2.5 wt.% Pd/Al_2O_3 with random macroporous structure.

Table 1
Surface areas of as-prepared Pd/Al_2O_3 catalysts with random macroporous structure

Catalyst	Surface area ($m^2\ g^{-1}$)
Al_2O_3	277.5
1.0 wt.% Pd/Al_2O_3	273.3
2.5 wt.% Pd/Al_2O_3	268.4
5.0 wt.% Pd/Al_2O_3	261.8

Fig. 7 shows methane conversion over Pd/Al_2O_3 catalyst with a random macroporous structure at different loading levels of Pd. It was found that the activity of Pd/Al_2O_3 rose with an increase in Pd content in the range of 1.0–2.5 wt.%. The catalytic activity improved very little when the Pd content increased further from 2.5 to 5.0 wt.%. Fig. 8 shows XRD patterns of the catalysts prepared with Pd contents of 1, 2.5, and 5.0 wt.%. When the concentration of Pd loading on the Al_2O_3 support was below 2.5 wt.%, the reflections of PdO were unclear because of the small particle size with low crystallinity. When the loading amount increased to 5 wt.%, PdO reflection peaks became clear and sharp because of the aggregation of small PdO particles. Comparing the catalytic activities of 2.5 wt.% Pd/Al_2O_3 with 5.0 wt.% Pd/Al_2O_3, we can consider that small PdO particles, dispersed on the support for 2.5 wt.% Pd/Al_2O_3 catalyst, could provide enough active sites and enhance catalytic activity for methane oxidation. Although the particle size of PdO was larger in 5.0 wt.% Pd/Al_2O_3 catalyst, it could also provide enough active sites for the reaction because the total amount of Pd was higher. As a result, both conditions showed almost the same catalytic activity. Table 1 indicates that Al_2O_3 powder prepared with a random macroporous structure had a BET surface area of 277.5 $m^2\ g^{-1}$. It should be noted that this kind of Al_2O_3 powder also contained large numbers of micropores, besides the macropores obtained from the PMMA particle template. Loading of Pd on this support could block some of the micropores on the framework, and reduce the total BET surface area. However, only about 5.7% of the surface area was reduced with 5.0 wt.% Pd/Al_2O_3 catalyst.

Long-term stability testing for methane combustion over 2.5 wt.% Pd/Al_2O_3 with a random macroporous structure was performed. As shown in Fig. 9, it was found that the catalyst showed stable behavior at 550 °C for 95 h, but the reactivity sharply decreased with the reaction time at 450 °C. When the reaction temperature increased to 550 °C after 180 h, the catalytic reactivity recovered to the initial state. It is possible that the incomplete combustion of methane at 450 °C in the microchannel for a long period could lead to the deposition of carbon on the catalyst surface, especially in the case of high concentration methane feed.

4. Conclusions

γ-Al_2O_3 catalyst supports with ordered and random macroporous structures and without macroporous structure were fabricated in microchannels. Pd catalysts with different concentrations were loaded using the incipient wetness impregnation method. Complete catalytic oxidation of high-concentration methane over the prepared catalysts in the microchannel reactor was investigated. The catalyst support with ordered macropore structure (inverse opal structure) had high porosity and highly uniform morphology in the microchannel, and showed the highest reactivity. However, the catalyst with random macroporous structure showed reactivity comparable to the catalyst with ordered macropore structure, and its fabrication process was very simple and easy. This indicated that introduction of macropores into the support by different methods can enhance catalytic reactivity in the microchannel reactor.

Acknowledgement

This study was supported by the Japan Society for the Promotion of Science (JSPS).

References

[1] C. Miesse, R.I. Masel, M. Short, M.A. Shannon, Proc. Combust. Inst. 30 (2005) 2499.
[2] C.M. Miesse, R.I. Masel, C.D. Jensen, M.A. Shannon, M. Short, AIChE J. 50 (2004) 3206.
[3] J. Han, D.Y. Zemlyanov, F.H. Ribeiro, Catal. Today 117 (2006) 506.
[4] S. Karagiannidis, J. Mantzaras, G. Jackson, K. Boulouchos, Proc. Combust. Inst. 31 (2007) 3309.
[5] V. Hessel, H. Löwe, A. Müller, G. Kolb, Chemical Micro Process Engineering—Processing, Applications and Plants, Wiley-VCH, Weinheim, Germany, 2005.
[6] G. Kolb, V. Hessel, Chem. Eng. J. 98 (2004) 1.
[7] B.E. Solsona, T. Garcia, C. Jones, S.H. Taylor, A.F. Carley, G.J. Hutchings, Appl. Catal. A: Gen. 312 (2006) 67.
[8] G. Lapisardi, L. Urfels, P. Gelin, M. Primet, A. Kaddouri, E. Garbowski, S. Toppi, E. Tena, Catal. Today 117 (2006) 564.
[9] H. Yoshida, T. Nakajima, Y. Yazawa, T. Hattori, Appl. Catal. B: Environ. 71 (2007) 70.
[10] C. Shi, L. Yang, J. Cai, Fuel 86 (2007) 106.
[11] K. Persson, A. Ersson, K. Jansson, N. Iverlund, S. Jaras, J. Catal. 231 (2005) 139.
[12] R. Kikuchi, S. Maeda, K. Sasaki, S. Wennerstrom, Y. Ozawa, K. Eguchi, Appl. Catal. A: Gen. 239 (2003) 169.
[13] K. Sekizawa, H. Widjaja, S. Maeda, Y. Ozawa, K. Eguchi, Appl. Catal. A: Gen. 200 (2000) 211.
[14] K. Eguchi, H. Arai, Appl. Catal. A: Gen. 222 (2001) 359.
[15] T. Takeguchi, O. Takeoh, S. Aoyama, J. Ueda, R. Kikuchi, K. Eguchi, Appl. Catal. A: Gen. 252 (2003) 205.
[16] G. Zhu, J. Han, D.Y. Zemlyanov, F.H. Ribeiro, J. Am. Chem. Soc. 126 (2004) 9896.
[17] M. Machida, H. Haniguchi, T. Kijima, J. Nakatani, J. Mater. Chem. 8 (1998) 781.
[18] O. Demoulin, M. Navez, E.M. Gaigneaux, P. Ruiz, A.-S. Mamede, P. Granger, E. Payen, Phys. Chem. Chem. Phys. 5 (2003) 4394.
[19] O. Demoulin, M. Navez, P. Ruiz, Appl. Catal. A: Gen. 295 (2005) 59.
[20] O. Demoulin, B. Le Clef, M. Navez, P. Ruiz, Appl. Catal. A: Gen. 344 (2008) 1.
[21] R. Zapf, C.B. Willinger, K. Berresheim, H. Bolz, H. Gnaser, V. Hessel, G. Kolb, P. Loeb, A.-K. Pannwitt, A. Ziogas, Trans. IChemE 81 (2003) 721.
[22] K. Haas-Santo, M. Fichtner, K. Schubert, Appl. Catal. A: Gen. 220 (2001) 79.
[23] I.-K. Sung, M. Christian, D. Mitchell, -P. Kim, P.J.A. Kenis, Adv. Funct. Mater. 15 (2005) 1336.
[24] Christian, M. Mitchell, D.–P. Kim, P.J.A. Kenis, J. Catal. 241 (2006) 235.

[25] Christian, M. Mitchell, P.J.A. Kenis, Lap Chip. 6 (2006) 1328.
[26] G. Guan, R. Zapf, G. Kolb, Y. Men, V. Hessel, H. Loewe, J. Ye, R. Zentel, Chem. Commun. (2007) 260.
[27] J.C. Ruiz-Morales, J. Canales-Vazquez, J. Pena-Martinez, D. Marrero-Lopez, J.T.S. Irvine, P. Nunez, J. Mater. Chem. 16 (2006) 540.
[28] F. Tang, H. Fudouzi, T. Uchikoshi, Y. Sakka, J. Eur. Ceram. Soc. 24 (2004) 341.
[29] F. Tang, H. Fudouzi, T. Uchikoshi, T. Awane, Y. Sakka, Chem. Lett. 32 (2003) 276.
[30] Y. Sakka, F. Tang, H. Fudouzi, T. Uchikoshi, Sci. Technol. Adv. Mater. 6 (2005) 915.